Applied Thermal Engineering 63 (2014) 1–10

Contents lists available at ScienceDirect

Applied Thermal Engineering

journal homepage: www.elsevier.com/locate/apthermeng

Analysis of a wooden pellet-fueled domestic thermoelectric cogeneration system

Kari Alanne*, Timo Laukkanen, Kari Saari, Juha Jokisalo

Department of Energy Technology, Aalto University, Espoo, Finland

HIGHLIGHTS

- A pellet-fueled thermoelectric cogeneration system is conceptualized and modeled.
- The performance of the system in a residential building in Finland is assessed.
- The electrical efficiency of 9% and temperature difference of 660 °C can be achieved.
- Maximum 47% of the building's annual electrical demand can be generated on-site.

ARTICLE INFO

Article history:
Received 6 June 2013
Accepted 26 October 2013
Available online 5 November 2013

Keywords:
Thermoelectric cogeneration
Biomass boiler
Residential micro-cogeneration

ABSTRACT

A domestic thermoelectric cogeneration system (DTCS) is a noiseless and maintenance-free method of on-site micro-cogeneration, with no moving parts. This paper contributes to the research by characterizing, modeling and assessing the performance of a DTCS, where thermoelectric modules are integrated directly in the combustion chamber of a wooden-pellet fueled boiler (nominal thermal output 20 kW_{th}), to keep structural changes minimal and the temperature difference large. The results suggest that temperature differences up to 660 °C can be achieved with the proposed configuration, the hot side temperature reaching the level of 750 °C (1023 K). The electrical output is 1.9 kW_e at most, and the electrical plant efficiency of 8.9% (LHV) can be obtained, when the figure of merit of the thermoelectric material is unity. Maximum 47% of the on-site electricity consumption can be met in a single-family house located in Finland. In comparison with a standard pellet-fueled boiler, the integrated DTCS is able to cut the annual non-renewable primary energy by 11% and CO_2 emissions by 21%. At present, the annual cost savings of 160 €/y at maximum can be achieved. To make the DTCS economically viable, further development of thermoelectric materials and better investment support is required.

1. Introduction

The present EU policy aims at a 20% cut of greenhouse gas emissions and a 20% proportion of renewable energy by 2020. According to Eurostat, households accounted for 26.7% of the final energy consumption in the EU-27 countries in 2010. Biomass has long traditions in heating and power generation. As renewable energy, it complements the exploitation of wind and solar PV/thermal as base-load energy supply, because it is a continuously available source of primary energy and also available on cold climatic areas during winter [1]. According to Dong et al. [1], the market potential of biomass-fueled micro-cogeneration technology has been recognized worldwide, but the level its commercialization and implementation is still low.

The key micro-cogeneration technologies within the smallest power range of 1–5 kW_e are fuel cells (FC), Stirling engines (SE), and internal combustion engines (ICE) [2]. The use of fuel cells and internal combustion engines is restrained either by their early stage of development (FC) or the need of fuel processing (e.g. gasification, reformation or electrolysis), easily resulting in extra costs, when biomass is utilized as a fuel [3]. Stirling engines (SE) raise to the challenge with their ability to utilize a variety of thermal sources [4]. Bonnet et al. [5] suggest the Ericsson engine as an alternative to SE due to its less complicated design and thus potentially reduced costs. Organic Rankine Cycle (ORC) has been considered a promising, low-cost alternative for biomass-fueled micro-cogeneration, capable of operating at low temperatures, which makes it suitable for waste heat recovery [6]. Alanne et al. [7] have proposed a rotary steam engine to be integrated with a 17 kW_{th} pellet-fueled boiler.

The possibility of recovering heat using thermoelectric generators has been studied since 1910s [8]. The first targets of application

* Corresponding author. Tel.: +358 50 4306837.
E-mail addresses: kari.alanne@aalto.fi, kalanne@iki.fi (K. Alanne).

1359-4311/$ – see front matter © 2013 Elsevier Ltd. All rights reserved.
http://dx.doi.org/10.1016/j.applthermaleng.2013.10.054

Nomenclature

A	overall heat transfer area, m^2
A_H	heat transfer area, m^2
$c_{p,G}$	specific heat of gas. J/kg K
$CO_{2fuel,i}$	carbon dioxide emission factor for the fuel into the system (i-th hour), g/kW h
$CO_{2grid,i}$	carbon dioxide emission factor for the grid electricity (i-th hour), g/kW h
d_h	hydraulic diameter (of the combustion chamber), m
h	convective heat transfer coefficient, W/m^2 K
h_{CW}	convective heat transfer coefficient of cooling water, W/m^2 K
h_G	convective heat transfer coefficient of gas, W/m^2 K
Nu	Nusselt number, −
P_{net}	net electrical power in AC, W
$PER_{fuel,i}$	primary energy factor for the fuel into the system (i-th hour), kW h/kW h
$PER_{grid,i}$	primary energy factor for the grid electricity (i-th hour), kW h/kW h
Pr	Prandtl number, −
$q_{m,G}$	mass flow of the combustion gases, kg/s
$Q_{fuel,i}$	fuel consumption of the micro-cogeneration system (i-th hour), kW h
Re	Reynolds number, −
S	Seebeck coefficient, μV/K
s_m	mean beam length of the thermal radiation, m
T	temperature, K
T_{ad}	adiabatic combustion temperature, K
T_C	heat sink temperature (cold side temperature of thermoelectric material), K
T_{CW}	average temperature of cooling water, K
T_G	gas temperature, K
$T_{G,ave}$	average gas temperature, K
T_H	hot source temperature (hot side temperature of thermoelectric material), K
T_{out}	gas outlet temperature from combustion chamber, K
ZT	figure of merit, −
$\overline{ZT}$	average figure of merit, −
V	volume (of the combustion chamber), m^3
$W_{grid,i}$	electricity purchased from the grid (i-th hour), kW h
α_G	absorptivity of combustion gases, −
α_{H_2O}	absorptivity of water vapor, −
α_{CO_2}	absorptivity of carbon monoxide, −
ε_G	emissivity of combustion gases, −
ε_H	emissivity of chamber wall, −
κ	electrical conductivity, S/m
λ	thermal conductivity, W/m K
σ	Stefan–Bolzmann constant, W/m^2 K^4
ε_G	emissivity of gas, −
Φ	heat flow, W
Φ_c	convective heat flow of combustion chamber, W
Φ_{cc}	total heat flow of combustion chamber, W
Φ_{cond}	conduction heat flow through the thermoelectric material, W
Φ_{CW}	heat flow to the cooling water, W
Φ_r	radiation heat flow of combustion chamber, W
Φ_{fuel}	thermal flow from fuel calculated from lower heating value (LHV), W
Φ_{th}	thermal flow delivered to the water circulation, W

were spacecrafts in 1950s [9]. Later, low-temperature difference (80–100 K) applications on off-shore oil platforms [10] and in heat recovery from solid waste [11] have been discussed. Stove-top applications for thermoelectric generators have been introduced by Killander & Bass [12] and Nuwayhid et al. [13], whereas Qiu & Hayden [14] present a natural gas-fired thermoelectric system. A conceptual domestic thermoelectric cogeneration system (DTCS) was introduced by Zheng et al. [15], who developed a bench-scale experimental prototype of a DTCS to be integrated in a domestic boiler system. Their target was to improve the electrical efficiency by better organizing the heat transfer and to avoid the use of a cooling fan, which was mentioned as a disadvantage in the stove applications. They achieved the conversion efficiency of 4% at the temperature difference of 130 °C and concluded that better performance can be obtained by a better design of heat exchangers. Their study did not address the boiler operation according to the user's needs and boiler size.

This paper conceptualizes a micro-cogeneration system, where thermoelectric material is directly integrated in the heat transfer surfaces of the combustion chamber and convection tubes of a conventional domestic wooden-pellet-fired boiler. The aim is to find the highest possible conversion efficiency with the slightest structural change in a commercial boiler. To that end, a computational model is developed to characterize the part-load electrical and thermal efficiencies (based on the lower heating value of the fuel, LHV) of the integrated system. The computational model can be applied to any boiler, any properties of fuel and any thermoelectric material. Secondly, a computational analysis is conducted to assess the cost and emission reduction potentials of a 20 kW_{th} DTCS. Both the daily operational hours and the annual energy balance of the DTCS in a typical single-family house in Finland are found out using the whole-building simulation tool IDA-ICE.

2. Theory

2.1. Thermoelectric modules

Thermoelectric power generation is based on the so called Seebeck effect, where a voltage is generated between two ends of N and P type semiconductors (thermoelectric materials). The voltage is proportional to the temperature difference between the ends of these semiconductors, where the hot end is connected to the thermal source (combustion) and the cold end to some heat sink (water circulation). The typical thermoelectric materials (bismuth in combination with antimony, tellurium or selenium) operate up to 523 K (250 °C), whereas some materials (alloys of lead telluride and silicon germanium) accept temperatures ranging from 850 to 1300 K (577–1027 °C) [15].

The semiconductors are arranged into thermoelectric modules (elements), where both the hot and the cold ends are attached to uniform heat transfer surfaces. In principle, by installing multiple elements on top of each other (multi-stage elements), the temperature difference between the hot and cold surfaces can be increased. The output of thermoelectric generation is direct current (DC) at the voltage level depending on how the thermoelectric modules are coupled (series and/or parallel). Power management unit (sine wave inverter) is required to convert the DC output to alternating current (AC) at desired voltage level (e.g. 220 V) and frequency (e.g. 50 Hz). The schematic diagram of thermoelectric power generation is in Fig. 1 and the structures of single and multi-stage thermoelectric modules are shown in Fig. 2.

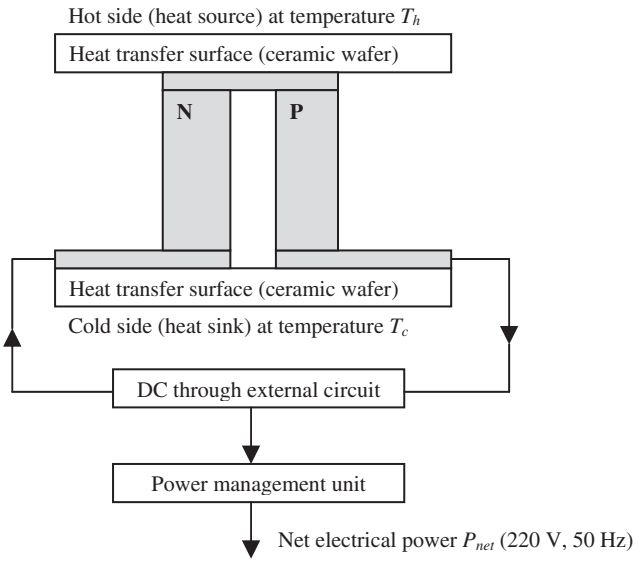

Fig. 1. Schematic diagram of thermoelectric power generation (single-stage).

2.2. The novel pellet-fueled DTCS concept

In standard pellet-fueled boilers, the combustion chamber is made of steel or another metal with a good thermal conductance and tolerance for high temperatures. The combustion chamber is surrounded by a body of circulated water. The temperature of exhaust gases drops significantly, before the gas exits from the combustion chamber. The remaining heat of exhaust gases is recovered in convection tubes after the chamber. The water is circulated and it can be stirred, which enables intensified forced convection from the outer surface of the combustion chamber to water.

When a standard boiler is converted into a domestic thermoelectric cogeneration system, the combustion chamber is either coated with thermoelectric modules or designed so that the heat transfer surface itself builds up one single water-proof thermoelectric structure. Here, the thermoelectric structure works as de facto insulator instead of conductor, and a multistage element is used to ensure as large temperature difference as possible. Exhaust gases exit from the combustion chamber at higher temperature, and a major part of the heat transfer now takes place in convection tubes after the chamber. The above principle is illustrated in Fig. 3.

The temperature of the water jacket at the top of the boiler is kept between lower and upper boundaries (80–90 °C) by the control (TC1) of the burner. The temperature of the supply water for the radiator network is controlled by mixing the return water from the radiator network with the hot boiler water, and the set point for the supply water temperature (max. 70 °C) is determined on the basis of outdoor temperature (TC2). Domestic hot water (55 °C) is also produced in the boiler, by circulating cold water through a heat exchanger located at the top of the boiler. Fig. 4 shows a schematic diagram of integrating the boiler into a hydronic heating system.

The power control is based on adjusting the fuel input to the burner. Several control strategies are useful, but basically the heat generation is adapted to track the thermal demand of the building, the electricity being a by-product of thermal supply. Here, excess electricity is fed into a battery or the power grid through the power conditioning system at the required AC/DC voltage, and the shortage is compensated by discharging the battery or purchasing electricity from the power grid.

3. Calculations

3.1. Performance of the thermoelectric module

The key temperatures for the energy conversion and heat transfer are depicted in Fig. 5.

The performance of any thermoelectric material is indicated by the figure of merit, ZT, which is calculated from Eq. (1) [15]:

$$\mathrm{ZT} = \frac{S^2 \kappa T}{\lambda} \tag{1}$$

where ZT is the figure of merit, T is temperature in Kelvin, S is the Seebeck coefficient, κ is the electrical conductivity and λ is the thermal conductivity.

The conversion efficiency of the thermoelectric structure is [15]

$$\eta_{\mathrm{TE}} = \frac{T_{\mathrm{H}} - T_{\mathrm{C}}}{T_{\mathrm{H}}} \left[\frac{\sqrt{1+\overline{\mathrm{ZT}}} - 1}{\sqrt{1+\overline{\mathrm{ZT}}} + \frac{T_{\mathrm{C}}}{T_{\mathrm{H}}}} \right] \tag{2}$$

where $\overline{\mathrm{ZT}}$ is the average figure of merit, T_{H} is the hot source temperature and T_{C} is the heat sink temperature in Kelvin.

3.2. Heat transfer in the combustion chamber and convection tubes

The major share of heat transfer in the combustion chamber takes place as radiation and is affected by the properties of carbon dioxide and water vapor in the combustion gases. Convection heat transfer dominates in cooling tubes, whereas the radiation plays a minor role only.

For the present model, the effective emissivity and absorptivity of carbon dioxide and water vapor are determined following the method presented by Stephan & Baehr [17]. In the present model, the combustion chamber is approximated as a cylinder with inclined top. The mean beam length of the thermal radiation in the chamber is $s_{\mathrm{m}} = 3.6\,(V/A)$ [17].

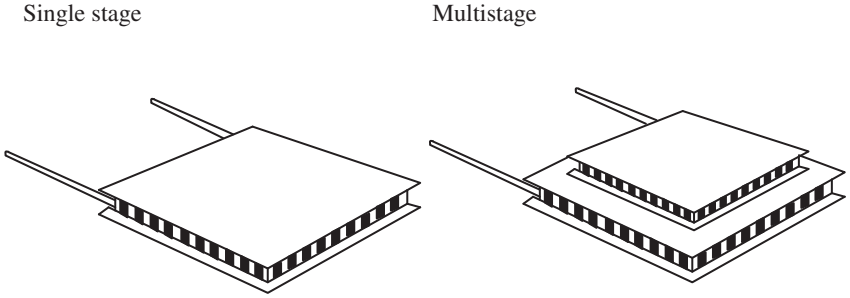

Fig. 2. Thermoelectric modules.

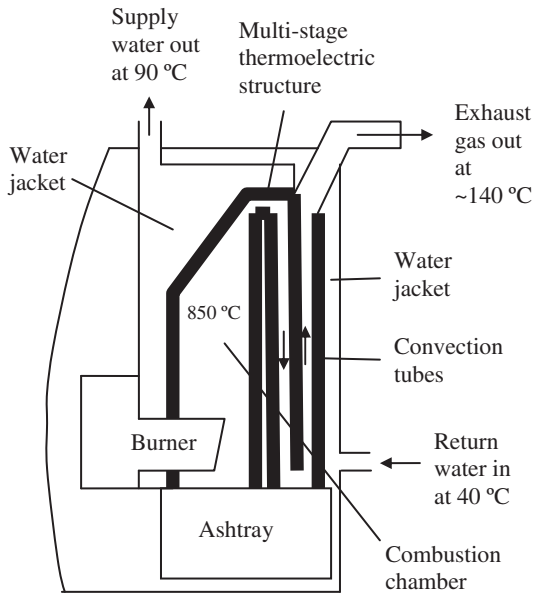

Fig. 3. Integrating thermoelectric structure into a pellet-fueled boiler.

The heat flow in the combustion chamber is calculated on the basis of heat capacity flow, adiabatic combustion temperature, and outlet temperature of combustion gases

$$\Phi_{cc} = q_{m,G} c_{p,G} (T_{ad} - T_{out}) \tag{3}$$

On the other hand, heat flow is the sum of radiation and convection heat flows

$$\Phi_{cc} = \Phi_r + \Phi_c \tag{4}$$

where radiation heat flow is calculated from

$$\Phi_r = \frac{\varepsilon_H + 1}{2} A_H \sigma \left(\varepsilon_G T_{G,ave}^4 - \alpha_G T_H^4 \right) \tag{5}$$

and convective heat flow from

$$\Phi_c = h_G A_H (T_{G,ave} - T_H) \tag{6}$$

where ε_H is the emissivity of the combustion chamber wall (the hot surface of the thermoelectric material), A_H is the heat transfer area of the combustion chamber, σ is Stefan-Bolzmann constant, ε_G is emissivity of the combustion gases, $T_{G,ave}$ T is the average gas temperature, α_G is the absorptivity of the combustion gases, T_H is the average chamber wall surface temperature (=hot side thermoelectric material surface temperature) and h_G is the convective heat transfer coefficient of the combustion gases [17].

The emissivity of the two molecular gases (H_2O and CO_2) is determined by the well-known Hottel-diagrams, where the temperature of the emitting gas, T_G, and the partial pressure of the gas multiplied by the mean beam length of the chamber ($p_G \cdot s_m$) are input parameters. The emissivity of water vapor is in addition corrected using a correction factor C_{H2O}, which depends on the partial pressure of the water vapor. When the emissivity of CO_2 is determined, the absorptivity of CO_2 can be calculated from

$$\alpha_{CO_2} = \varepsilon_{CO_2} (T_G / T_H)^{0.65} \tag{7}$$

Correspondingly, for H_2O absorptivity

$$\alpha_{H_2O} = \varepsilon_{H_2O} (T_G / T_H)^{0.45} \tag{8}$$

Relying on Eq. (5), the emission of the gases is proportional to the 4th power of absolute gas temperature T_G. Thus, the emitting average gas temperature in the combustion chamber $T_{G,ave}$ is calculated based on adiabatic combustion temperature and outlet temperature

$$T_{G,ave}^4 = \frac{1}{T_{out} - T_{ad}} \int_{T_{ad}}^{T_{out}} T^4 dT = \frac{T_{out}^5 - T_{ad}^5}{5(T_{out} - T_{ad})} \tag{9}$$

Combining the Eqs. (3)–(6) and (9), the heat flow from the gases is in the combustion chamber can be calculated from

$$\Phi_{cc} = q_{m,G} c_{p,G} (T_{ad} - T_{out}) = \frac{\varepsilon_H + 1}{2} A_H \sigma \left(\varepsilon_G T_{G,ave}^4 - \alpha_G T_H^4 \right) + h_G A_H (T_{G,ave} - T_H) \tag{10}$$

The above heat flow is conducted through the thermoelectric material to the cooling water side. The conduction heat flow through the material is

$$\Phi_{cond} = \frac{\lambda_e}{\delta_e} A_H (T_H - T_C) \tag{11}$$

where λ_e is the heat conductivity and δ_e the thickness of thermoelectric structure. T_C is the average cooling water side surface temperature of the thermoelectric structure.

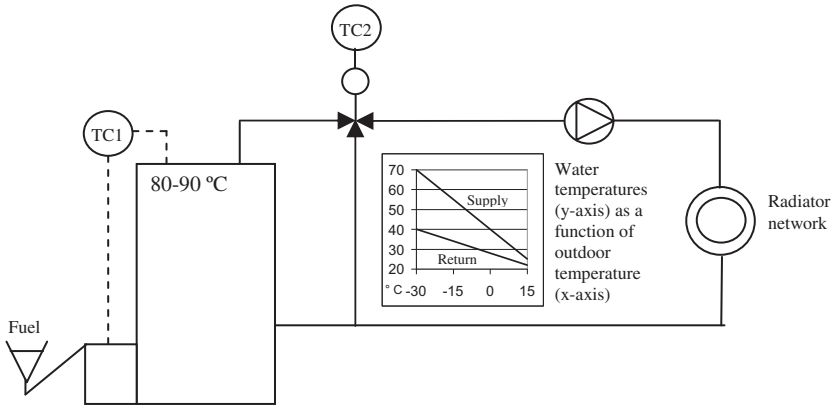

Fig. 4. Schematic diagram of a hydronic heating system [16].

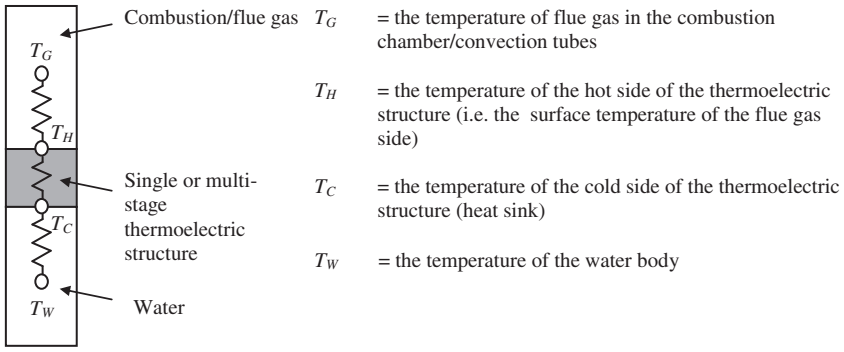

Fig. 5. Temperature profile of the energy conversion in DTCS.

Finally, heat flow transferred to the cooling water is

$$\Phi_{CW} = h_{CW}A_C(T_C - T_{CW})(= \Phi_{cond}) \quad (12)$$

where h_{CW} is the convective heat transfer coefficient of cooling water, including the heat transfer resistance of thin metallic chamber wall. T_{CW} is the average temperature of cooling water. Because no heat is stored to the system, the total heat flow from the combustion chamber is transferred through conduction and convection, a fraction of it converted to electricity and a fraction transferred to cooling water, which can be expressed as

$$\Phi_{cc} = \Phi_r + \Phi_c = \Phi_{CW} + \eta_{TE}\Phi_{cc} \quad (13)$$

The convective heat transfer coefficients for both the combustion chamber and for the water body are determined in terms of the Nusselt number (Nu): $h = Nu \cdot (\lambda/d_h)$. The required correlation for the combustion chamber is

$$Nu = 0.664\sqrt{(Re)}Pr^{1/3} \quad (14)$$

and for the gas flow in cooling tubes

$$Nu = 1.8(RePr(d_h/L))^{1/3} \quad (15)$$

The Nusselt number for the water side is calculated from the well-known Dittus–Boelter correlation:

$$Nu = 0.023Re^{0.8}Pr^{0.4} \quad (16)$$

where the flow speed on the water side of 5 cm/s is used.

The heat flow in the convection tubes, Φ_{ct}, is calculated basically in the same way as in the combustion chamber The main difference is that the average gas temperature is now the arithmetic average of the inlet and outlet temperatures. No combustion takes place, when the inlet temperature of convection tubes equals to the outlet temperature of combustion chamber.

3.3. Plant efficiency and part-load operation

The overall performance of the integrated DTCS is evaluated in terms of electrical, thermal and overall efficiencies. The efficiencies of the integrated system are defined in Eqs. (17)–(19):

$$\text{Electrical efficiency } \eta_e = \frac{P_{net}}{\Phi_{fuel}} \quad (17)$$

$$\text{Thermal efficiency } \eta_{th} = \frac{\Phi_{th}}{\Phi_{fuel}} \quad (18)$$

$$\text{Overall efficiency } \eta_{tot} = \frac{P_{net} + \Phi_{th}}{\Phi_{fuel}} \quad (19)$$

In the above definitions, Φ_{fuel} is the thermal flow from fuel calculated from lower heating value (LHV), Φ_{th} is the thermal flow delivered to the water circulation (taking into account the heat losses through exhaust gases and the envelope of the boiler), and P_{net} is the net electrical power in AC (including the losses of power management system).

Correspondingly, the net electrical power and thermal flow delivered to the water circulation are defined in Eqs. (20) and (21).

$$P_{net} = \eta_{PM}\eta_{TE}\Phi_{tot} \quad (20)$$

$$\Phi_{th} = (1 - \eta_{TE})\Phi_{tot} \quad (21)$$

where η_{PM} is the efficiency of the power management system.

The part-load operation is brought about by adjusting the pellet feed-in mechanism so that the fuel input represents a certain fraction of the nominal fuel capacity. Part-load ratio is defined as

$$r = \Phi_{fuel}/\Phi_{fuel,nom} \quad (22)$$

where $\Phi_{fuel,nom}$ represents the 100% fuel capacity of the boiler. Here, convective heat transfer coefficients are assumed to be proportional to the flow Reynolds numbers as shown in Eqs. (14)–(16). The effect of mass flow changes in part load conditions now can be taken into account, when calculating the heat transfer coefficient.

3.4. Primary energy use and CO_2 emission rates

The primary energy use and CO_2 emission rates are calculated by summing up the products of simulated hourly consumptions of each energy carrier (fuel, electricity) and the corresponding energy conversion factors (PE or CO_2). The annual (8760 h) primary energy demand Q_{pr} is now

$$Q_{pr} = \sum_{i=1}^{8760}\left(Q_{fuel,i}PER_{fuel,i} \pm W_{grid,i}PER_{grid,i}\right) \quad (23)$$

where $Q_{fuel,i}$ and $W_{grid,i}$ are the fuel consumption of the micro-cogeneration system and the electricity purchased from the grid, and $PER_{fuel,i}$ and $PER_{grid,i}$ are the primary energy factors for the fuel consumed by the system and the grid electricity during the i-th hour. Correspondingly, the carbon dioxide emissions are obtained from

$$CO_2 = \sum_{i=1}^{8760}\left(Q_{fuel,i}CO_{2fuel,i} \pm W_{grid,i}CO_{2grid,i}\right) \quad (24)$$

where $CO_{2fuel,i}$ and $CO_{2grid,i}$ are the carbon dioxide emission factors for the fuel used by the system and the grid electricity during the i-th hour. In Eqs. (23) and (24), the purchased electricity $W_{grid,i}$ is negative, when surplus electricity is fed into the grid at the i-th hour.

3.5. Computational analysis

3.5.1. Target boiler

The computational analysis is applied to a common, pellet-fueled hydronic boiler (Ariterm Biomatic 20+) with nominal thermal output of 20 kW_{th}. The performance of the reference boiler has been tested against the European Standard EN 303-5, Clause 4.1 by the Technical Research Centre of Finland (VTT). The test report is confidential. The boiler data is summarized in Table 1.

The integrated DTCS makes use of the same body as the above pellet boiler, but the combustion chamber and the convection tubes (which are made of 5 mm steel plate in the standard boiler) are now assumed to have been replaced by thermoelectric structure (thickness varying from 1 to 4 cm). For the computational performance analysis, a constant ZT-value and thermal conductivity of the material are assumed, which resembles the properties of Bi_2Te_3.

3.5.2. Target building

The target building is a one-floor single-family house located in Helsinki, Finland. The building is equipped with a central mechanical exhaust ventilation system with no heat recovery. The heating system is programmed to maintain a constant room temperature. The building does not contain a cooling system, allowing the temperature to rise during summer months. The electrical demand is the sum of the power requirements of appliances (including fans and pumps) and lighting. The hourly profile is estimated on the basis of everyday experience. The annual level of electrical consumption is acquired from Haulio [18]. The daily demand profiles of electricity used for lighting have been determined separately for each season: winter (October to February), spring (March and April), summer (May to July), and autumn (August and September). The electrical demand profiles are shown in Fig. 6.

Table 1
Input data for the computational analysis.

Fuel	
Pellet diameter [mm]	8
Moisture content [%]	8.6%
Calorific value [MJ/kg]	17.25
Boiler/DTCS	
Net weight (empty) [kg]	245
Gross (installed) dimensions [mm]	935 × 608 × 1755
Heat transfer area of combustion chamber [m^2]	0.72
Heat transfer area of convection tubes [m^2]	1.35
Water volume [L]	140
Measured boiler efficiency (LHV) at nominal thermal load [%]	91%
Measured boiler efficiency (LHV) at 30% thermal load [%]	86%
ZT-value	1
Thermal conductivity of thermoelectric structure [W/m K]	1.2
Simulated building	
Weather file	Helsinki–Vantaa Int'l Airport (1980–2009)
Heated area [m^2]	135.6
Number of occupants	4
Occupied each day between	5:00 P.M.–8:00 A.M.
Air flow rate [L s^{-1}]	49.5 (constant air flow)
Daily hot water demand [L]	240
Room temperature [°C]	21.5
U-value (walls) [W/m^2 K]	0.42
U-value (windows) [W/m^2 K]	2.2
U-value (floor) [W/m^2 K]	0.3
U-value (ceiling) [W/m^2 K]	0.24

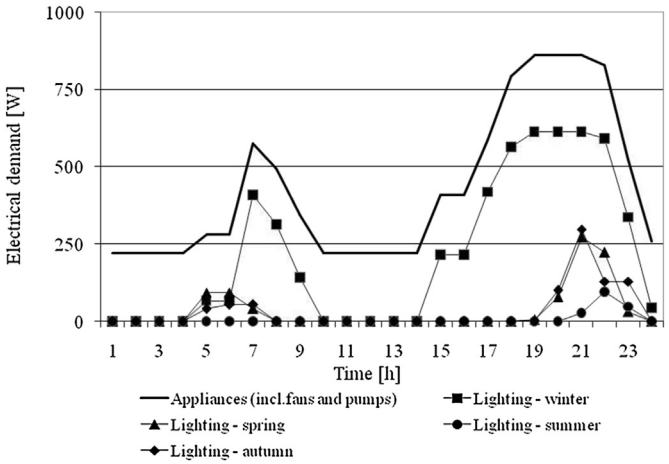

Fig. 6. Daily profiles of electrical demand.

The demand of domestic hot water is evaluated, relying on the general estimate that four occupants consume 60 L per person per day [19]. The specific water flow of a tap and a shower is 0.2 L/s [20], and the estimate of the Finnish Energy Agency (Motiva) for the proportion of hot water in the total water consumption is 40%. The water is heated from 5 °C to 55 °C [19]. Assuming that showers are in use 5 min at 7:00 A.M., 8:00 P.M., 9:00 P.M. and 10:00 P.M. and the taps 10 min at 6:00 A.M., 6:00 P.M. and 11:00 P.M, the total consumption of hot water is 240 L. Outside the heating period, thermal energy is still needed to produce hot water, and a high temperature must be maintained in the boiler. In stand-by conditions, heat transfer between the boiler and the surrounding air (skin losses) must be compensated. The summary of the key input data for building simulation is in Table 1. The reader is referred to Kalamees et al. [21] for further details.

3.5.3. Research method

The IDA-ICE whole-building simulation tool, which has been validated for example in Travesi et al. [22] and Loutzenhiser et al. [23] are employed in combination with a spreadsheet-based post-processing application to determine the operational hours, the electric power shortage and surplus for a single-family house equipped with a pellet-fueled, integrated DTCS. In validity tests, the variation between actual energy demand and energy demand estimated on the basis of dynamic, whole-building simulations has been observed to be up to ±10%, but the best agreements lay within ±3% [24].

The operation of the DTCS is modeled in accordance with the principles depicted in Section 3. The parameters of the model are calibrated to full agreement with the experimental measurement conducted by VTT for the standard boiler. The electricity conversion losses are neglected. The skin loss from the boiler to the room is considered small in comparison with the exhaust losses. The power demand of the water circulation pump and the heat gain related to integrated boiler skin losses are considered the same as them of the standard boiler.

The boiler operates in thermal-tracking mode, i.e. the thermal energy demands are met and electricity is considered a "by-product". Two operational strategies are examined. In the first strategy, the boiler is controlled following the "on–off"-mode, where the hourly thermal demand is compensated by running the burner at nominal (100%) fuel input (thermal output) as long as needed. In the second strategy, the boiler operates at three power levels: 100%, 65% or 30%, according to the hourly average thermal requirements.

The ON/OFF controlled boiler operates at nominal (design) power when the system is switched on. In that case, the fuel feeding

mechanism is fully open or closed and the fuel input corresponds to the nominal (100%) fuel capacity. The thermal flow transferred to water circulation is referred to as nominal thermal power of the system. The net electrical output in the same conditions is the nominal electrical output of the system.

4. Results and discussion

4.1. Temperatures and efficiencies

With the reference fuel, the adiabatic combustion temperature was calculated for all the examined power levels, being 1480 °C at the 100% operation. The calculation method was the thermal engineering software PROSIM (Endat – Thermal Power Plant Simulations, Website: http://www.endat.fi/, last access, October 9, 2013). The temperatures of the exiting exhaust gases (T_G) and the temperature difference over the thermoelectric structure were determined through the thermodynamic model in Section 3. The results for both the combustion chamber and the convection tubes are summarized in Table 2 for the nominal (100%) operation. The thickness zero (0 cm) of thermoelectric structure refers to the standard boiler, where the combustion chamber has been made of 5 mm steel.

As seen in Table 2, temperature differences up to 660 °C can be achieved using the present configuration, the hot side temperature reaching the level of 750 °C (1023 K). In these conditions, the use of thermoelectric materials with tolerance to high temperatures, such as lead telluride and silicon germanium, is required. Since the used ZT value is conservative, the present study to some extent underestimates the electrical output of the system in high temperatures.

Because the thermoelectric structure works as an insulation between the combustion chamber and the water envelope, the exhaust gas will leave the boiler at a relatively high temperature, which increases the heat loss. Running the standard boiler at the nominal power, the exhaust gases can be cooled down to 100 °C, whereas with the 4 cm thermoelectric structure thickness, the flue gas temperature will remain as high as 200 °C. Correspondingly, the heat flow to the water is reduced, which has to be taken into account when selecting a DTCS for heating purposes. In the present study, the size of the boiler was sufficient to satisfy the heating demand of the building in all circumstances.

The electrical and thermal efficiencies of the examined DTCS are in Fig. 7. The efficiencies are given for both the nominal operation (100%) and the part-load operations (30% and 65%) as a function of the material thickness. The upper (descending) curves represent the thermal efficiencies and the lower (progressive) curves the electrical efficiencies.

Table 2
Temperature profiles of the DTCS.

Thickness of thermoelectric structure [cm]	Temperatures [°C]			
	T_G	T_H	T_C	Temperature difference
Combustion chamber				
0	592.5	125.0	125.0	0.0
1	640.7	281.9	116.4	165.4
2	741.0	428.2	106.6	321.6
3	810.1	594.0	98.8	495.2
4	907.5	748.0	88.5	659.5
Convection tubes				
0	104.0	90.1	90.1	0.0
1	131.0	132.9	83.2	49.7
2	156.0	177.5	80.7	96.8
3	178.0	216.0	78.3	137.7
4	203.0	260.1	75.8	184.2

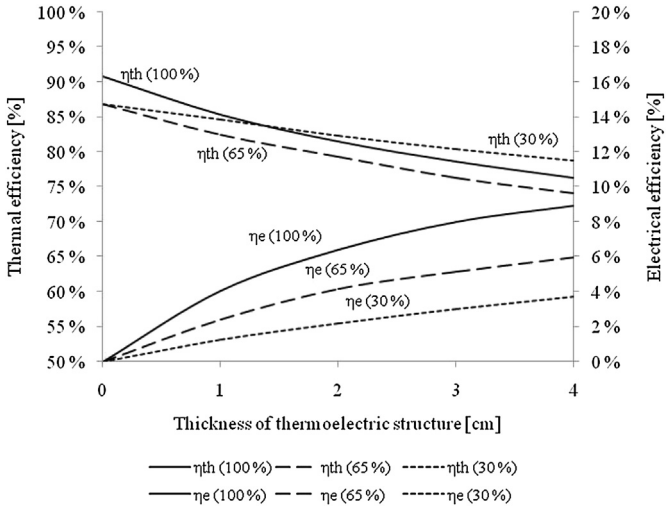

Fig. 7. Electrical and thermal efficiencies of the DTCS (full load and part-load).

The maximum electrical plant efficiency (8.9%) is obtained at 4 cm structure thickness. The corresponding nominal electrical output is 1.91 kW_e, the majority of which taking place in the thermoelectric structure installed in the combustion chamber. Due to the insulation effect of the thermoelectric structure, the overall efficiency (i.e. the sum of electrical and thermal efficiencies) will be reduced. When operated at the nominal power, the O_2 concentration in the exhaust gases is 6%. At the part load, increased amount of combustion air remains without participating in the combustion. Thus, the O_2 concentration in the exhaust gases is 10% at 65% load and 14% at the 30%, load, which, in turn, decreases the efficiency. Here, the efficiencies have been determined for the above part loads only. The DTCS is operable at any part load between 20% and 100% and the corresponding efficiencies can be determined by the model in Section 3.

4.2. Annual energy balance and operational hours

The building's simulated annual electrical demand is 4719 kW h/y and thermal demand (including both space heating and domestic hot water) is 26,319 kW h/y. The proportions of the annual purchased and delivered electrical energy for each thermoelectric structure thicknesses are depicted in Fig. 8. The graph also indicates which part of the annual electrical energy consumption can be met through the DTCS (on-site).

The data indicates that maximum 47% of the annual electrical consumption can be met using the on-off-controlled DTCS (at 4 cm structure thickness, annual operating hours 1608 h/y). Significant annual electrical surplus can be achieved only if the structure thickness is 3 cm or more. The annual fuel consumptions (solid line) and operational hours (dashed line) are illustrated in Fig. 9.

Generating electricity with the pellet-boiler still ensuring that enough heat will be transferred to the hydronic heating system increases both the number of operational hours and the fuel consumption of the DTCS. This is because an equal nominal fuel input is used for both the standard boiler and the DTCS. Controlling the boiler at three power levels drastically increases the annual operational hours, but also results in the part-load operation at lower thermal efficiency. As a consequence, higher fuel consumption occurs than in the on-off operation, but no significant amount of electricity is generated. Hence, the further analysis for savings in primary energy, costs and emissions are conducted for the on-off operated DTCS only.

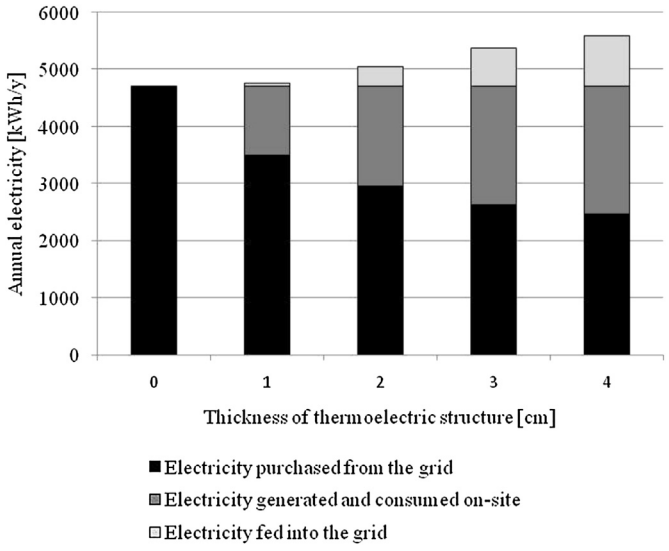

Fig. 8. Electrical energy balance for the on–off-controlled DTCS.

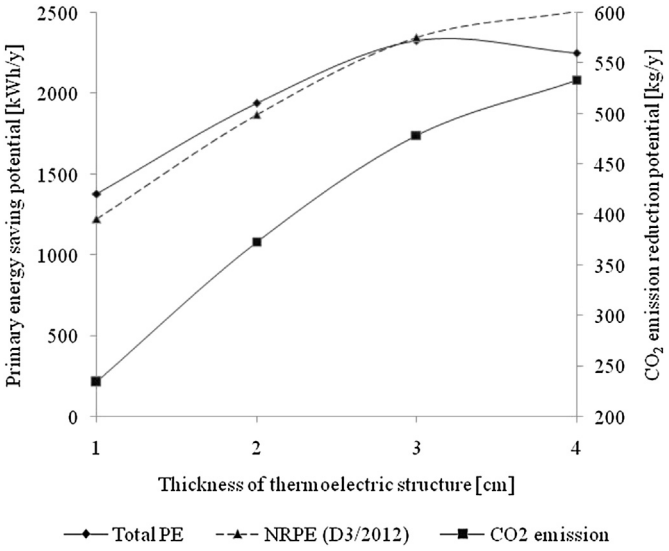

Fig. 10. Primary energy and CO_2 emission reduction potentials.

4.3. Reduction potentials for primary energy and CO_2 emissions

Two data acquirement methods have been used for primary energy and CO_2 emission factors to find out the reduction potentials. In the first method, the hourly total primary energy factors and CO_2 emission factors are acquired from the Finnish electricity production mix for the year 2006, provided by Finnish Energy Industries (ET), and the total primary energy factor of 1.14 kW h/kW h and the CO_2 emission factor of 43 g/kW h for wooden pellet are used [25]. In the second method, the non-renewable primary energy (NRPE) factors (constant throughout a year) for local bio-fuels (0.5) and electricity (1.7) are used as reference. The latter method follows the latest Finnish Building Code D3, 2012 [26]. The reduction potentials for each thickness of thermoelectric structure in the on-off controlled DTCS are visualized in Fig. 10.

The data in Fig. 10 implies that increasing the thickness of thermoelectric material from 1 cm to 2 cm has a more significant impact on the reduction potential than increasing the thickness from 3 to 4 cm. In compliance with these results, three centimeters seems to be a close-to-optimum material thickness for a DTCS in terms of reducing the total primary energy. For thicknesses more than that, the increasing fuel consumption starts to nullify the benefits obtained from the generated electricity. The maximum reduction potentials (4 cm structure thickness) in proportional terms are 5% for total primary energy, 11% for non-renewable primary energy, and 21% for CO_2 emissions.

In Finland, wooden pellet boilers are commonly purchased by private consumers to replace obsolete oil-fueled boilers. The customer would have to decide whether to replace the boiler by a standard pellet-fueled boiler or by a DTCS. According to D3 [26], the non-renewable primary energy factor for light fuel oil is 1.0 and the CO_2 emission factor of 261 g/kW h has been used in the instructions to the Finnish Energy Agency Motiva for a single target building. In the above conditions, replacing an oil-fueled boiler (annual efficiency 81% LHV) by a DTCS with 3 cm thermoelectric structure would cut the non-renewable primary energy consumption from 41 MW h/y to 20.5 MW h/y, which defrays a 50% reduction. The corresponding numbers for CO_2 emission reductions are from 9736 kg/y to 2031 kg/y and 79%. It is worth mentioning, however, that only replacing the oil-fueled boiler with a standard pellet-fueled boiler already cuts the NRPE by 44% and CO_2 by 74%.

According to Pellettienergia.fi, there are some 70,000 oil-heated single-family dwellings in Finland that could be potentially heated by a pellet-fueled boiler. Given that the simulated house represents relatively well an existing Finnish single-family house, the estimated maximum nationwide non-renewable primary energy reduction potential (replacement of an oil-heated boiler by a DTCS with 3 cm thermoelectric structure) would be 1420 GW h/y, and the CO_2 emission reduction potential would be 540,000 t/y.

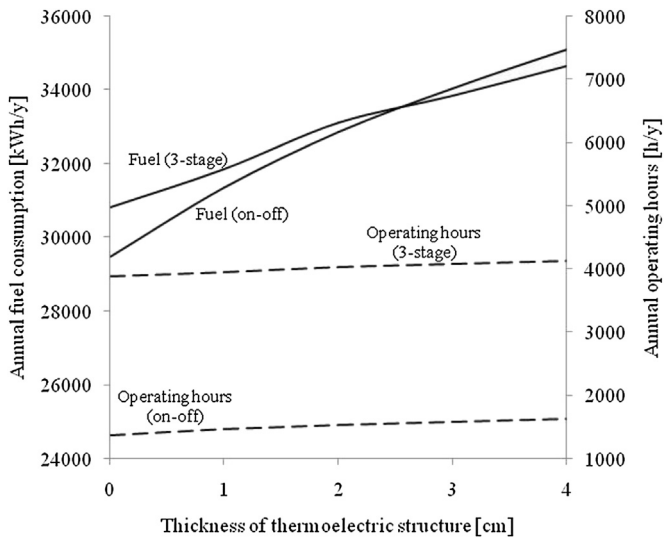

Fig. 9. Fuel consumption and annual operating hours for the DTCS.

4.4. Annual cost saving potentials

The cost saving potential is calculated by multiplying the annual energy consumption of each energy carrier (fuel, electricity) by a specific retail price. For electricity, the average market price in May, 2013 in Finland was 15.3 c/kW h according to the Energy Market Authority. Correspondingly, the average retail price for wooden pellet was 5.6 c/kW h according to Statistics Finland (2012). The total annual cost for electricity in the reference case (all electricity purchased from the grid) is in these conditions 722 €/y and the total fuel cost 1630 €/y.

In Finland, there is no feed-in tariff for electricity fed into the grid. Therefore, the sensitivity of the cost saving potential to the buyback price of electricity has been investigated instead of assigning fixed values. Here, the buyback price varies in the range 0 c/kW h and 15 c/kW h. This range is based on an unpublished survey of 15 EU countries, which was carried out at Aalto University Dept. of Energy Technology in 2011 making use of national renewable energy action plans of the Member States of the European Union. The survey concluded that the average feed-in tariff for small electricity generation based on biomass was 10.5 c/kW h at minimum and 12.6 c/kW h at maximum.

The results suggest that significant cost savings (more than 100 €/y) can be obtained only, if the DTCS is on–off operated. On the other hand, a feed-in tariff (or a net-metering scheme) is necessary to enable a monetary compensation of electricity fed into the grid. The annual cost savings in comparison with the standard boiler for each thickness of thermoelectric structure and four buyback prices of electricity (0, 5, 10 and 15 c/kW h) are summarized in Fig. 11.

The data indicate that increasing the thickness of the thermoelectric structure beyond 3 cm does not improve the economic benefit of the system. The explanation to this is the role of fuel consumption and generated electricity in the same way as mentioned in Section 4.3.

4.5. Economic viability

The maximum allowable difference (extra) costs for the DTCS in comparison with the standard boiler structure were assessed. A three centimeter thermoelectric structure thickness was chosen with an assumption that cost recovery period longer than five years is not acceptable. The discount rate (real interest rate) was allowed to vary in the range 3–10% and the impact was examined at the buyback rates of 0, 5, 10 and 15 c/kW h. The allowable difference cost intervals at cost recovery period of five years are shown in Fig. 12.

The data in Fig. 12 are the representation of the condition of economic viability, i.e. if the difference cost remains at the given level (or below that), the investment is feasible. At present, a set of 56 mm × 56 mm thermoelectric modules (max. operational temperatures 250–300 °C, without the costs of installation) can be ordered at the roughly price of 7600 €/m^{2}at minimum [27]. In the present application, a thermoelectric structure (combustion chamber and convection tubes) at this price level would cost up to 15,000 €. The difference between a DTCS and a standard boiler is not only the thermoelectric structure, but a power management system with backup-batteries is also required. The average price (of six retailers) for a sine wave inverter (inverting 12 VDC to 240 VAC, 50 Hz at the power of 1500 W) in Finland is 490 €. Assuming that the backup electrical storage would require two 180 Ah batteries (total storage capacity 4 kWh), their extra cost would be roughly 500 € [28]. At the above price levels, the total difference costs would be up to 16,000 €, and upgrading a standard boiler to a DTCS apparently would not be economically feasible.

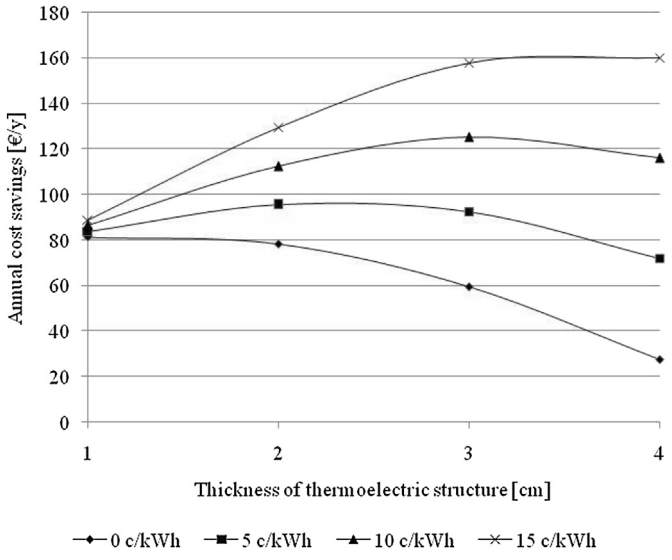

Fig. 11. Annual cost saving potentials (on–off operation).

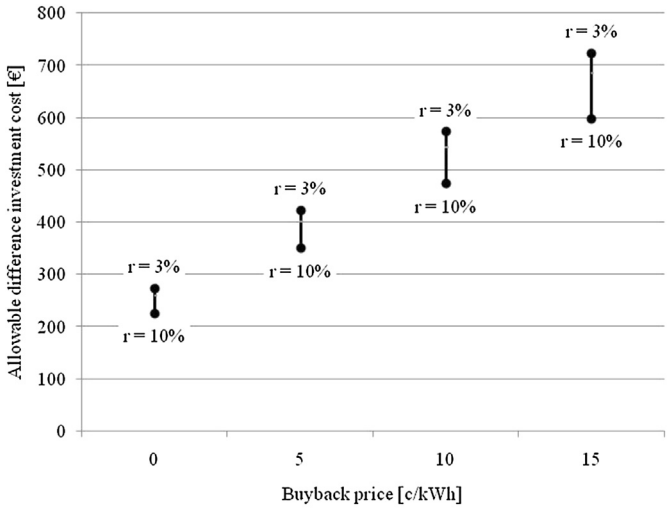

Fig. 12. Allowable difference costs at cost recovery period 5 years.

According to the Finnish Ministry of Environment, a household in Finland may receive a governmental support covering up to 20% of the capital investment. In the international context, the governmental support for biomass-fueled small-scale (<100 kW$_e$) cogeneration may be up to 60%, but this open-handed supports are ordinarily targeted to larger than domestic-scale plants. Assuming, for example, a 20% investment support for the DTCS and no investment support for the standard boiler (reference price 5716 €), the allowable cost of 3 cm thermoelectric structure (at 5 years cost recovery period) would be 660 €/m^2 depending on the buyback rate. This is only 4% of the price of commercially available thermoelectric modules (7600 €/m^2).

The above cost estimates are based on the retail prices of one of the present commercial thermoelectric modules. In practice, these are not optimal for the proposed purpose, because their insufficient tolerance for high temperatures. The benefits related to the mass-production of boilers with integrated DTCS have not been accounted for, either. For these reasons, the cost estimates are rather illustrative than realistic. However, the above data provide a signpost for the expected price development of thermoelectric materials and governmental strategies to promote the introduction of biomass-based energy supply in domestic use.

5. Conclusions

This paper conceptualized a micro-cogeneration system, where thermoelectric material is directly integrated in the heat transfer surface of the combustion chamber of a conventional domestic wooden-pellet-fired boiler. To that end, a computational model was developed to characterize the part-load electrical and thermal efficiencies (based on the lower heating value of the fuel, LHV) of the integrated system. The heat transfer model is applicable for any

thermoelectric material. A computational analysis was conducted to assess the cost and emission reduction potentials of a 20 kW_{th} DTCS in a single-family house in Finland.

It was found that temperature differences up to 660 °C can be achieved with the proposed configuration, the hot side temperature reaching the level of 750 °C (1023 K). The electrical output of the plant is 1.9 kW_e at most, and the electrical efficiency of 8.9% (LHV) can be obtained, when the figure of merit (ZT) of the thermoelectric material is unity. The results revealed that maximum 47% of the on-site electricity consumption can be met, the operational hours being 1608 h/y. In contrast, the values for a corresponding micro-cogeneration system based on a rotary-steam engine were 31% and 1274 h/y [7]. In comparison with a standard pellet-fueled boiler, the integrated DTCS was able to cut the annual non-renewable primary energy by 11% and CO_2 emissions by 21%. The annual cost savings of 160 €/y at maximum can be achieved. The present approach is applicable to the analysis of similar pellet-fueled DTCS and the results can be generalized to cold climates in similar operational conditions.

In the computational analysis, the figure of merit (ZT) and the thermal conductivity were selected according to the properties of bismuth–telluride. This selection was made because the material is commercially available and a realistic (conservative) conception of the performance of the DTCS was sought for. In practice, tolerance for higher temperatures would be required than what bismuth-telluride has. At present, the total electrical output relatively was deposited restrained, even though large temperature differences were achieved.

In the future, low-cost thermoelectric modules should be developed in terms of both improved figure of merit and better tolerance for high temperatures. The integration of the thermoelectric material into pellet-fueled boilers will also require further development. The multi-stage structure should be made of several materials optimized in accordance with their life-cycle costs, performance and tolerance for given temperature levels. To that end, the thermodynamic model proposed in this work requires further development. The future research also calls for experimental testing in both laboratory and in the field, to find out its performance in realistic conditions. To allow extended operational hours during the cooling period, applications such as micro-scale poly-generation with DTCS and absorption cooling would be worth investigation.

Acknowledgements

The exchange of information between Ariterm Oy, Pelletienergia.fi and Aalto University Dept. of Energy Technology is gratefully acknowledged.

References

[1] L. Dong, H. Liu, S. Riffat, Development of small-scale and micro-scale biomass-fuelled CHP systems – a literature review, Appl. Therm. Eng. 29 (2009) 2119–2126.
[2] M. Denticed'Accadia, M. Sasso, S. Sibilio, L. Vanoli, Micro-combined heat and power in residential and light commercial applications, Appl. Therm. Eng. 23 (2003) 1247–1259.
[3] R.C. Brown, C. Stevens, Thermochemical Processing of Biomass: Conversion into Fuels, Chemicals and Power, John Wiley & Sons Ltd, New York, NY, USA, 2011. ISBN: 978-0-470-72111.
[4] V. Dorer, A. Weber, Energy and CO_2 emissions performance assessment of residential micro-cogeneration systems with dynamic whole-building simulation programs, Energy Convers. Manag. 50 (2009) 648–657.
[5] S. Bonnet, M. Alaphilippe, P. Stouffs, Energy, exergy and cost analysis of a micro-cogeneration system based on an Ericsson engine, Int. J. Therm. Sci. 44 (2005) 1161–1168.
[6] S. Quoilin, S. Declaye, B.F. Tchanche, V. Lemort, Thermo-economic optimization of waste heat recovery Organic Rankine Cycles, Appl. Therm. Eng. 31 (2011) 2885–2893.
[7] K. Alanne, K. Saari, M. Kuosa, J. Jokisalo, A.R. Martin, Thermo-economic analysis of a micro-cogeneration system based on a rotary steam engine (RSE), Appl. Therm. Eng. 44 (2012) 11–20.
[8] J.C. Bass, N.B. Elsner, F.A. Leavitt, Performance of the 1 kW Thermoelectric generator for diesel engines, in: 13th International Conference on Thermoelectrics, Kansas City, NO, American Institute of Physics, New York, 1995, pp. 295–298.
[9] D.M. Rowe, United States thermoelectric activities in space, in: Proceedings VIII Int Conf. on Thermoelectric Energy Conversion, Nancy, France, 10–13 July 1989, pp. 133–142.
[10] D.M. Rowe, Thermoelectric conversion of waste heat from redundant oil wells, in: Proceedings Mediterranean Petroleum Conf, 1992, pp. 556–563.
[11] T. Kajikawa, I. Makoto Ito, I. Katsube, E. Shibuya, Development of thermoelectric power generation utilising heat of combustible solid waste, in: B. Mathiprakasam (Ed.), Proc. of the 13th Int. Conf. on Thermoelectrics, Kansas City Mo, 1994, pp. 314–318.
[12] A. Killander, J. Bass, A stove-top generator for cold areas, in: Proc. of the 15th Int. Conf. on Thermoelectrics, Pasadena, USA, 1996, pp. 390–393.
[13] R.Y. Nuwayhid, D.M. Rowe, G. Min, Low cost stove-top thermoelectric generator for regions with unreliable electricity supply, Renew. Energy 28 (2003) 205–222.
[14] K. Qiu, A.C.S. Hayden, A natural-gas-fired thermoelectric power generation system, J. Electron. Mater. 38 (7) (2009) 1315–1319.
[15] X.F. Zheng, Y.Y. Yan, K. Simpson, A potential candidate for the sustainable and reliable domestic energy generation–Thermoelectric cogeneration system, Appl. Therm. Eng. 53 (2013) 305–311.
[16] O. Seppänen, Rakennusten lämmitys (Heating of buildings), in Finnish, Suomen LVI-liitto (Finnish Society of Heating, Ventilation and Air-Conditioning), Helsinki, Finland, 2001.
[17] H.D. Baehr, K. Stephan, Heat and Mass Transfer, Springer, Berlin Heidelberg, Germany, 2006, ISBN 978-3-540-29526-6.
[18] M. Haulio, Sähkönkulutuksen analysointi ja mallintaminen kerrostaloissa (Modeling and analysis of electricity consumption of apartment buildings), in Finnish (Master's thesis), Department of Energy Technology, Helsinki University of Technology, Espoo, 2009.
[19] Finnish Ministry of the Environment, Section D5 of the National Building Code of Finland – Calculation of Performance and Energy Requirement for the Heating of Buildings, 2007. Helsinki.
[20] Finnish Ministry of the Environment, Section D1 of the National Building Code of Finland – Calculation of Performance and Energy Requirement for the Heating of Buildings, 2007. Helsinki.
[21] T. Kalamees, K. Jylhä, H. Tietäväinen, J. Jokisalo, S. Ilomets, R. Hyvönen, S. Saku, Development of weighting factors for climate variables for selecting the energy reference year according to the EN ISO 15927-4 standard, Energy Build. 47 (2013) 53–60.
[22] J. Travesi, G. Maxwell, C. Klaassen, M. Holtz (Eds.), Empirical Validation of Iowa Energy Resource Station Building Energy Analysis Simulation Models, 2001. IEA Task 22, Subtask A, Ames, IA, USA.
[23] P. Loutzenhiser, H. Manz, G. Maxwell, Empirical Validations of Shading/Daylighting/Load Interactions in Building Energy Simulation Tools, 2007. A Report for the International Energy Agency SHC Task 34, ECBCS Annex 43 Project C, Ames, IA, USA.
[24] P. Tuomaala, Implementation and Evaluation of Air Flow and Heat Transfer Routines for Building Simulation Tools (Doctoral thesis), Helsinki University of Technology, Espoo, 2002.
[25] R. Frischknecht, U. Bollens, S. Bosshart, M. Ciot, L. Ciseri, G. Doka, R. Dones, U. Gantner, R. Hischier, A. Martin, Ökoinventare von Energiesystemen: Grundlagen für den ökologischen Vergleich von Energiesystemen und den Einbezug von Energiesystemen in Ökobilanzen für die Schweiz, in: Bundesamt für Energie (Ed.), Gruppe Energie – Stoffe – Umwelt (ESU), Auflage No. 3, Eidgenössische Technische Hochschule Zuerich und Sektion Ganzheitliche Systemanalysen, Paul Scherrer Institut, Villigen, 1996. Bern.
[26] Finnish Ministry of the Environment, Section D3 of the National Building Code of Finland – Energy Efficiency of Buildings, 2012. Helsinki.
[27] TEG – Thermoelectric Gencell Technology, web site: http://www.tecteg.com (last accessed 9.10.2013).
[28] Suntekno, web site: http://www.suntekno.fi, (last accessed 9.10.2013).